agronomy

MDPI

Article

Effects of Irrigation Schedules on Maize Yield and Water Use Efficiency under Future Climate Scenarios in Heilongjiang Province Based on the AquaCrop Model

Tangzhe Nie [1], Yi Tang [1], Yang Jiao [1], Na Li [1], Tianyi Wang [1,2], Chong Du [1,*], Zhongxue Zhang [2,3], Peng Chen [4], Tiecheng Li [2,3], Zhongyi Sun [5] and Shijiang Zhu [6]

1 School of Water Conservancy and Electric Power, Heilongjiang University, Harbin 150080, China; 2019036@hlju.edu.cn (T.N.); ty979794@163.com (Y.T.); jiaoyang0814@163.com (Y.J.); L17863523371@163.com (N.L.); wangtianyi7176@163.com (T.W.)
2 School of Water Conservancy and Civil Engineering, Northeast Agricultural University, Harbin 150030, China; zhangzhongxue@163.com (Z.Z.); litiecheng1212@126.com (T.L.)
3 Key Laboratory of Efficient Use of Agricultural Water Resources, Ministry of Agriculture and Rural Affairs, Northeast Agricultural University, Harbin 150030, China
4 College of Agricultural Science and Engineering, Hohai University, Nanjing 210098, China; chenpeng_isotope@163.com
5 College of Ecology and Environment, Hainan University, Haikou 570208, China; gis.rs@hainanu.edu.cn
6 College of Hydraulic and Environmental Engineering, China Three Gorges University, Yichang 443002, China; zhusjiang@aliyun.com
* Correspondence: duchong@hlju.edu.cn; Tel.: +86-136-3366-1083

check for updates

Citation: Nie, T.; Tang, Y.; Jiao, Y.; Li, N.; Wang, T.; Du, C.; Zhang, Z.; Chen, P.; Li, T.; Sun, Z.; et al. Effects of Irrigation Schedules on Maize Yield and Water Use Efficiency under Future Climate Scenarios in Heilongjiang Province Based on the AquaCrop Model. *Agronomy* **2022**, *12*, 810. https://doi.org/10.3390/agronomy12040810

Academic Editors: Pantazis Georgiou and Dimitris Karpouzos

Received: 3 March 2022
Accepted: 26 March 2022
Published: 27 March 2022

Publisher's Note: MDPI stays neutral with regard to jurisdictional claims in published maps and institutional affiliations.

Abstract: Predicting the impact of future climate change on food security has important implications for sustainable food production. The 26 meteorological stations' future climate data in the study area are assembled from four global climate models under two representative concentration pathways (RCP4.5 and RCP8.5). The future maize yield, actual crop evapotranspiration (ET_a), and water use efficiency (*WUE*) were predicted by calibrated AquaCrop model under two deficit irrigation (the regulated deficit irrigation (RDI) at jointing stage(W1), filling stage(W2)), and full irrigation (W3) during the three periods (2021–2040, 2041–2060, and 2061–2080). The result showed that the maize yields under W1, W2, and W3 of RCP4.5 were 2.8%, 2.9%, and 2.5% lower than those in RCP8.5, respectively. In RCP8.5, the yield of W3 was 1.9% and 1.4% higher than W1 and W2, respectively. Under the RCP4.5, the ET_a of W1, W2, and W3 was 481.32 mm, 484.94 mm, and 489.12 mm, respectively. Moreover, the ET_a of W1 was significantly lower than W2 under the RCP4.5 and RCP8.5 ($p > 0.05$). In conclusion, regulated deficit irrigation at the maize jointing stage is recommended in the study area when considering *WUE*.

Keywords: maize; AquaCrop; actual crop evapotranspiration (ET_a); yield; water use efficiency (*WUE*); irrigation schedule; climate change

1. Introduction

Climate change has a great impact on agricultural systems. [1]. Climate change, characterized by temperature rise, the uncertain amount and patterns of precipitation (*Pe*), and elevated atmospheric CO_2 concentration [2], is a widely concerned issue in global development [3]. According to the Intergovernmental Panel on Climate Change (IPCC), the future temperature will increase by 1.5 °C or higher, particularly significant in the high latitudes and tropical regions [4]. In order to maintain the stable development of the agricultural economy and food security, it is necessary to predict the impact of future climate change on crop growth [5]. Due to sustaining the needs of the increasing population, the modern era model would replace the traditional model. Crop models would be one of the tools of future agricultural research. A well-efficient and validated model can be used to optimize resources and predict the yield [6].

With the temperature increasing, fluctuations in both amount and frequency of *Pe* and changes in CO_2 concentration would all directly impact crop evapotranspiration, actual evapotranspiration (ET_a), and irrigation water requirements [7]. With the crop growing, potential evapotranspiration and net irrigation water requirements would decrease if CO_2 concentrations increased [8]. Furthermore, the high temperature can actively promote the growth of most crops, advance crop phenology, shorten crop growth period, and reduce the cumulative biomass of crops, thus affecting the final yield [9,10]. Crop yields may vary due to climate change impacts in different regions, the region's latitude, and irrigation applications [11]. The maize's yield under normal, critical, and minimum irrigation in the North China Plain varied between 10,964–11,235 kg/ha [12]. In the Adana region, the highest maize yield (10,075 kg/ha) was obtained when irrigation limits were set between 25% ready water available (RAW) depletion and field capacity (FC), while the lowest yield (9837 kg/ha) was obtained when irrigation limits were set between 100% RAW depletion and FC [13]. However, many scholars proposed water-saving irrigation schedules to cope with the challenge of water shortage to ensure food security [14].

Water use efficiency (WUE) is an index for rational selection of irrigation schedule. Regulated deficit irrigation (RDI) is beneficial to yield increase by studying the effects of different water-deficit treatments on yield, ET_a, and *WUE* [15]. Appropriate water deficit treatment at the maize jointing stage can dramatically improve the utilization rate of irrigation water, and maize will not reduce production but improve maize yield traits [16]. When water deficit was affected in transpiration by reducing the irrigation and wet surface soil time, the ET_a would be decreased. RDI will generally have lower *WUE* than full irrigation [17]. Due to the uncertainty of the future climate, the crops may suffer water stress, and future yields would be unstable. Exploring the impact of different RDI schedules on maize for seed production under future climate conditions is very important for optimizing irrigation schedules and crop production selection. Volk et al. [18] forecasted the maize yield in Tanzania under the future climate, and they concluded that the establishment of different RDI schedules had no significant effect on maize yield. Jalil et al. [19] found that a reasonable selection of RDI system was of benefit to increasing the *WUE* and yield of winter wheat. However, there are relatively few studies on how to avoid yield loss by adjusting the deficit irrigation at each growth stage of crops under future climate scenarios.

Maize has played a significant role in meeting global food requirements and its yield accounts for nearly 30% of total global food production. According to the Food and Agriculture Organization of the United Nations (FAO) report, 23% of the world's maize yield comes from China, and China's maize harvested area accounts for more than one-fifth of the worldwide. Heilongjiang Province is an essential commercial grain base in China. Maize is the largest food crop in Heilongjiang Province, and its plant area and yield rank first in China. In 2019, the plant area of maize in the province was 5.87 million ha, and the yield was 39.4 billion kg [20]. Climate will seriously affect the growth of maize yield due to the uneven distribution of climate in Heilongjiang Province in the future [21]. It is necessary to combine rain-fed and RDI to ensure basic food security.

AquaCrop is an agricultural model that could reliably simulate maize yields under different irrigation schedules [22]. The AquaCrop model is sensitive to the water stress module. The simulation process has fewer steps and simple input parameters, which make the AquaCrop model widely used [23]. The AquaCrop model accurately simulated maize yield over some ranges. When assessing maize yield under different water stress irrigation schedules in semi-arid regions, compared to 50% field capacity irrigation, the AquaCrop model could more accurately simulate maize yield under 75% field capacity irrigation and full irrigation [24]. AquaCrop simulations have high accuracy in maize yield under full irrigation in the North China Plain. Under full irrigation, the error was 5% and 6% for grain yield and biomass, respectively. The error of full irrigation is smaller than that of rainfed. However, the model could be used to simulate maize yield and biomass under full irrigation [25]. Aquacrop was widely used in agricultural forecasting production around the world [26–28].

Studying the **optimal** selection of maize yield, ET_a, and *WUE* under different irrigation schedules in Heilongjiang under future climate changes will effectively provide optimal irrigation schedules for future maize planting systems. Our aims of this study were 1. to localize AquaCrop model parameters using observational data from irrigation experiments in the study region; and 2. to apply the calibrated model to evaluate the impacts of three irrigation schedules on maize yield and *WUE* in Heilongjiang Province under future climate scenarios.

2. Materials and Methods

2.1. Study Site and Field Data Sources

The research site is located in Heilongjiang Province in Northeast China, which is between 43°26′ and 53°33′ in latitude and 121°11′ and 135°05′ in longitude (Figure 1). The average temperature was between 3.1~4.6 °C, and the average annual *Pe* mainly was between 400 and 650 mm. *Pe* was concentrated primarily in June-August. The 6th accumulated temperature zone in Heilongjiang Province was unsuitable for maize planting. Thus, we didn't study the 6th accumulated temperature zone.

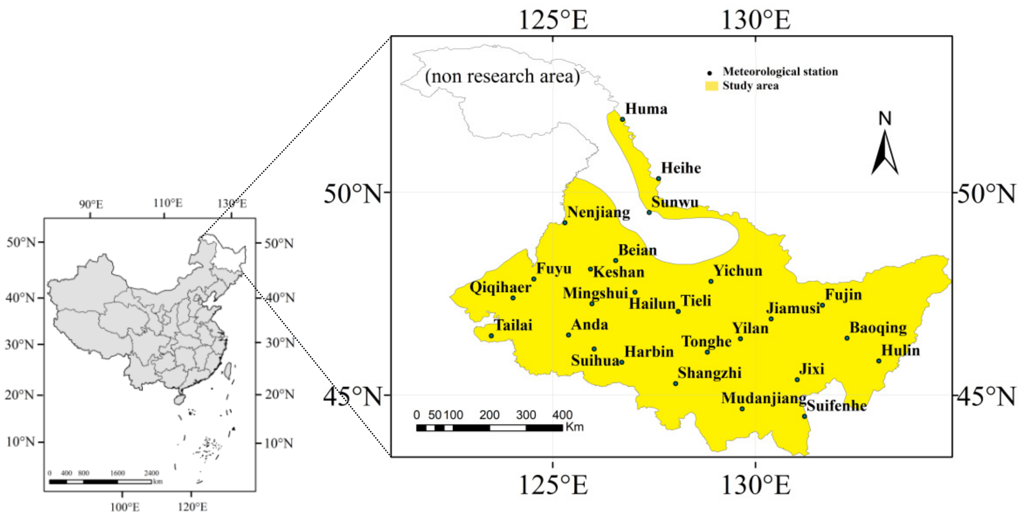

Figure 1. Locations of the Heilongjiang Province and 26 meteorological stations.

The field data of this study are from a four-year experiment established in the National Irrigation Experimental Center (45°43′09′′ N, 126°36′35′′ E, and altitude 140 m) in Harbin, Heilongjiang Province. The soil texture is loam, and the basic soil properties are as follows: N, 154.4 mg/kg; P_2O_5, 40.1 mg/kg; K_2O, 376.8 mg/kg; and pH, 7.27 [29]. We choose the maize growing four periods (emergence stage, jointing stage, tasseling stage, and filling stage) to study the effect of water stress at different growth stages on maize yield and ET_a (Table 1). A rain shelter was used to control precipitation. The size of each test pit used was 2.5 m × 2 m × 1.7 m.

Table 1. Irrigation treatments from 2014 to 2017.

Year	Treatments	Irrigation Upper and Lower Limit in Different Growth Stages of Maize (% of FC)			
		Emergence Stage	Jointing Stage	Tasseling Stage	Filling Stage
2014	T1	80–100%	50–100%	80–100%	80–100%
	T2	80–100%	80–100%	80–100%	50–100%
	T3	80–100%	80–100%	80–100%	80–100%
2015	T4	80–100%	45–100%	80–100%	80–100%
	T5	80–100%	80–100%	80–100%	45–100%
	T6	80–100%	80–100%	80–100%	80–100%
	T7	100%	100%	100%	100%
2016	T8	60–70%	70–80%	70–80%	70–80%
	T9	70–80%	50–60%	70–80%	70–80%
	T10	70–80%	70–80%	70–80%	70–80%
2017	T11	60–70%	70–80%	70–80%	70–80%
	T12	50–60%	70–80%	70–80%	70–80%
	T13	70–80%	70–80%	70–80%	70–80%

Note: Number before "–" in the table represents the lower limit of irrigation, and number after "–" in the table represents the upper limit of irrigation. "80–100%" in T1 treatment represents the irrigation starts when the soil moisture content reached 80% FC (the lower limit of irrigation), and the irrigation stops until the soil moisture content reached 100% FC (the upper limit of irrigation). Other explanations are the same as above. T8, T11, and T12 represent RDI treatments during the emergence stage; T1, T4, and T9 represent RDI treatments during the jointing stage; T2 and T5 represent RDI treatments during the filling stage; T3, T6, T7, T10, and T13 represent full irrigation treatments of maize growth. FC is the field capacity.

2.2. Future Climate Data

The Global Climate Model (GCM) is a tool used to study the earth's climate. In the Coupled Model Intercomparison Project phase 5, more than 60 GCMs have been proposed to contribute to future climate research [30]. In order to avoid the unreliability of a single GCM, multiple models were used to collect the predicted data of GCMs [31]. However, the future climate data were based on the ensemble datasets of four GCMs under the RCP4.5 and the RCP8.5, respectively. This study selected 26 meteorological stations distributed in different places in the Heilongjiang Province (Figure 1). Meteorological data consist of the daily maximum temperature (*Tmax*), daily minimum temperature (*Tmin*), *Pe*, and *Rad* from 2021 to 2080. We used the LARS-WG random weather generator downscaling method to generate future climate scenarios [32]. The calibration and verification data of the LARS-WG was derived from the historical meteorological data of daily *Tmax*, *Tmin*, *Pe*, and *Rad* of 26 meteorological stations from 1960 to 2015. The output meteorological data were the daily *Tmax*, *Tmin*, *Pe*, and *Rad* of four GCMs (Table 2) under RCP4.5 and RCP8.5, respectively, from 2021 to 2080. The period from 2021 to 2080 is divided into three research stages 2030s (2021–2040), 2050s (2041–2060), and 2070s (2061–2080). For details of the downscaling method, refer to [33]. The output meteorological data will be input into the AquaCrop. RCP8.5 represents radiation forcing values of more than 8.5 W/m^2 in 2100, and RCP4.5 means 4.5 W/m^2 when stable after 2100 [34]. We focus on the selection of RCP4.5 and RCP8.5 based on the socioeconomic conditions of radiative forcing currently faced by humans [35].

Table 2. 4 GCMs datasets in the LARS-WG model.

GCMs	Research Center	Countries and Regions	Grid Resolution
EC-EARTH	EC: Earth Consortium	Europe	1.125° × 1.125°
HadGEM2-ES	United Kingdom(UK) Meteorological Office	UK	1.25° × 1.88°
MIROC5	The University of Tokyo, National Institute for Environmental	Japan	1.39° × 1.41°
MPI-ESM-MR	Max Planck Institute for Meteorology	Germany	1.85° × 1.88°

2.3. AquaCrop Model Introduction and Settings

The AquaCrop model input data includes four modules, which are the climate module, crop module, management module, and soil module. Climate data includes daily *Tmax*, *Tmin*, *Pe*, *Rad*, and reference evapotranspiration (ET_0). The ET_a is calculated by ET_0-calculator software [36]. The crop data input section has some default values for crops growth parameters in this module. We need to adjust the corresponding plant parameters (including plant each growth period, sowing date, etc.) based on different climate and research sites. The crop growth was determined based on 14 agrometeorological observation stations in Heilongjiang Province. For the meteorological station without observation data, the data of the neighboring agrometeorological observation station in the same accumulated temperature area is selected as the calculation basis [37]. In order to improve the accuracy of output data during model simulation, parameters should be adjusted appropriately according to specific conditions. Irrigation management is specified by the irrigation method and the irrigation events. The irrigation schedule is formulated according to the irrigation time and depth of each stage of the crop growth period [14]. Soil data that describe soil properties in each layer are from The Soil Science Database (http://vdb3.soil.csdb.cn/, accessed on 30 March 2021).

To avoid the confounding effect of the non-productive consumptive water use (soil evaporation), the AquaCrop model calculates crop transpiration (*Tr*), soil evaporation (*E*), and ET_a using the following equation:

$$T_r = K_s K_{s_{Tr}} \left(K_{c_{Tr,x}} CC^* \right) ET_0 \tag{1}$$

$$E = K_r (1 - CC^*) K_{ex} ET_0 \tag{2}$$

$$ET_a = T_r + E \tag{3}$$

where, CC^* is the adjusted actual canopy coverage (%); $K_{C_{Tr,x}}$ is the maximum standard crop transpiration coefficient (dimensionless); K_S means the water stresses coefficient (dimensionless); $K_{S_{Tr}}$ is the temperature stresses coefficient (dimensionless); ET_0 is the reference evapotranspiration (mm); K_r is the evaporation reduction coefficient (dimensionless); K_{ex} is the maximum soil evaporation coefficient (dimensionless). ET_a was separated into *Tr* and *E* (mm).

In this study, the method recommended by FAO-66 was used to calculate the maize yield and *WUE*. As:

$$Y = f_{HI} HI_0 B \tag{4}$$

$$WUE = Y/ET_a \tag{5}$$

where *Y* is maize yield (kg/ha). f_{HI} is the harvest index adjustment factor (dimensionless). HI_0 is a reference harvest index (dimensionless), which means the yield ratio to biomass, *B* means the aboveground dry (kg/ha), *WUE* means water use efficiency (kg/m^3).

In this study, the inverse distance weighting (IDW) and Kriging methods of ArcGIS were used to interpolate the numerical values of each station output by AquaCrop into the study area, to analyze the spatial characteristics of the effects of different irrigation schedules on maize yield, ET_a, and *WUE* in Heilongjiang Province under future climate. The two-factor ANOVA of SPSS Statistics 17 was used to test the difference in yield, ET_a and *WUE* under different irrigation schedules.

In this study, we explored the effects of water stress at maize different growth stages on maize development. The generation of irrigation schedules in the AquaCrop model was used to evaluate or design a particular irrigation schedule. Irrigation practice was generated according to the specified time and a depth criterion when the model was running. In this study, RDI was set and generated at a specific time; the depth of irrigation depends on whether the soil moisture content reaches the set irrigation lower limit. When the soil moisture content falls to the set minimum limit, it will automatically irrigate to the fixed upper limit. The growth stage of maize is divided into four stages: emergence, jointing, tasseling, and filling. The jointing and filling stages of maize are essential stages of nutrient generation in crop growth [38]. Therefore, we set up three irrigation schedules, full irrigation and deficit irrigation in two crucial growth periods of maize. The three irrigation schedules sets are W1: water stress treatment in maize jointing stage. The lower and upper limits are 50% FC and 80% FC, respectively; W2: water stress treatment in maize filling stage. The lower and upper limits are 50% FC and 80% FC, respectively; W3: full irrigation schedule, which made maize suffer no water stress in the entire growth cycle.

2.4. AquaCrop Calibration and Verification

We selected the experimental data to calibrate the yield and ET_a in two years (2014–2015) main RDI (T1, T2, T3, T4, T5, T6, T7). Validation data were established by the six main RDI (T8, T9, T10, T11, T12, T13) experimental data from 2016 to 2017. The statistical parameters, including normalized RMSE ($CV(RMSE)$), determination coefficient (R^2), Willmott's agreement index (d), and model efficiency coefficient (EF) were determined for the performance evaluation of AquaCrop.

$$R^2 = 1 - \frac{\sum(\mathrm{yi} - \hat{\mathrm{yi}})^2}{\sum(\mathrm{yi} - \hat{\mathrm{y}})^2} \tag{6}$$

$$CV(RMSE) = \frac{1}{\bar{\mathrm{O}}}\sqrt{\frac{\sum(\mathrm{Pi} - \mathrm{Oi})^2}{\mathrm{n}}} \tag{7}$$

$$d = 1 - \frac{\sum(\mathrm{Pi} - \mathrm{Oi})^2}{\sum\left(\left|\mathrm{Pi} - \bar{\mathrm{O}}\right| + \left|\mathrm{Oi} - \bar{\mathrm{O}}\right|\right)^2} \tag{8}$$

$$EF = \frac{\sum_{\mathrm{i}=1}^{\mathrm{n}}\left(\mathrm{Oi} - \bar{\mathrm{O}}\right)^2 - \sum_{\mathrm{i}=1}^{\mathrm{n}}(\mathrm{Si} - \mathrm{Oi})^2}{\sum_{\mathrm{i}=1}^{\mathrm{n}}\left(\mathrm{Oi} - \bar{\mathrm{O}}\right)^2} \tag{9}$$

where yi is the actual value, ŷi is the simulated value, and ŷ is the mean value. And Ō is the mean observations, pi is the simulated value, and Oi is the observed value. n means the research count. A simulation can be considered perfect if $CV(RMSE)$ is smaller than 10%, good if between 10 and 20%. d range is 0–1, with 0 indicating a bad fit and 1 indicating a good fit between the simulated and observed data. The EF value is smaller than 1; a positive value indicates that the simulated value better describes the measured data trend than the mean observations.

The flow chart showing the optimal selection of future irrigation schedules using the AquaCrop model is provided in Figure 2.

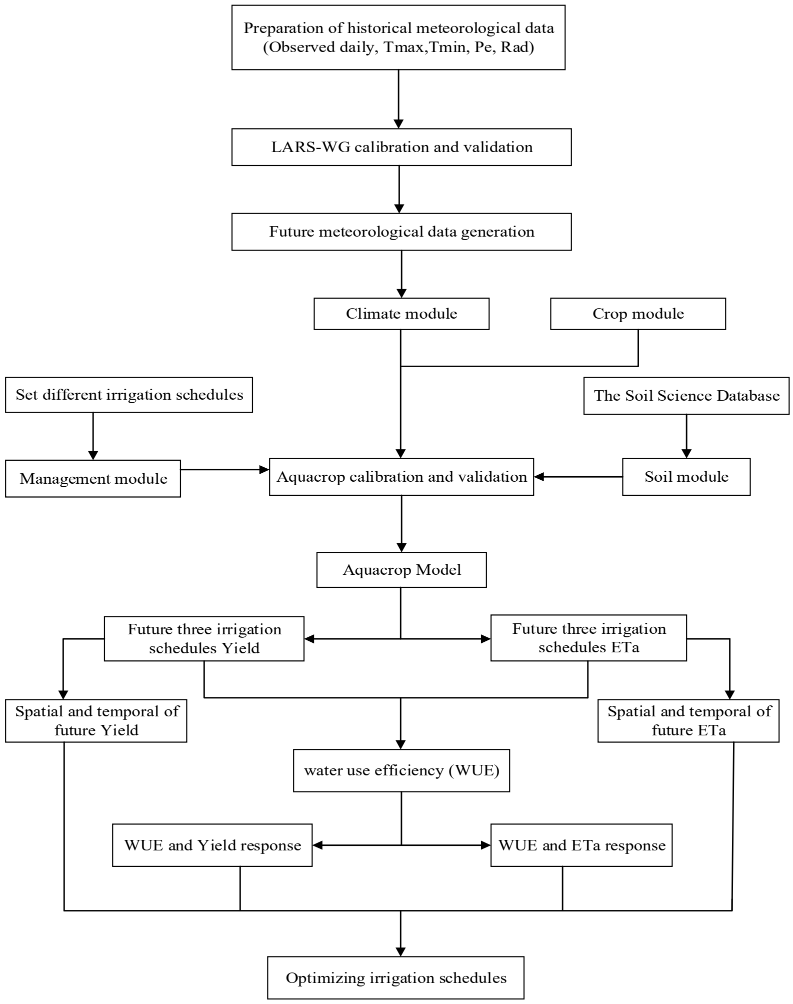

Figure 2. Flow chart for the steps involved in the estimation of future irrigation schedules using the AquaCrop model.

3. Results

3.1. Performance Evaluation of AquaCrop

Based on the AquaCrop model calibration and verification of the ET_a and yield, the model-simulated different irrigation schedules ET_a and yield agree well with the field-observed (Table 3). The R^2 of the simulated and observed maize yield reaches 0.72, and the average difference between simulated and observed yield under different treatments did not exceed 200 kg/ha (Figure 3). Each difference of the simulated and observed ET_a was less than 50 mm (Figures 4 and 5). When calibrating the AquaCrop model, the simulated and measured values of maize in different RDI were well fitted (Figure 4). From the six treatments in the validation, the model is reasonable in simulating the ET_a of the maize (Figure 5). Therefore, the AquaCrop model simulation results on maize ET_a and yield under different irrigation schedules during the whole growth stage were reliable and applicable for this study area.

Table 3. Fit indexes of AquaCrop model-simulated and measured ET_a and yield.

Parameter	*CV* (*RMSE*) (%)	*d*	R^2	*EF*
ET_a	8.21	0.99	0.97	0.97
Yield	4.44	0.91	0.72	0.68

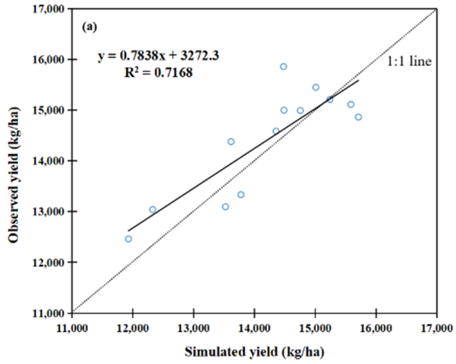

Figure 3. Calibration and validation of the AquaCrop model with yield (2014–2017).

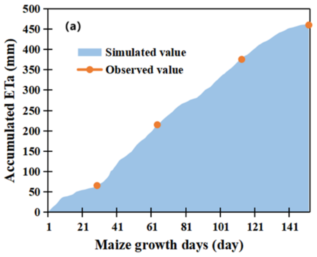

(a) T1

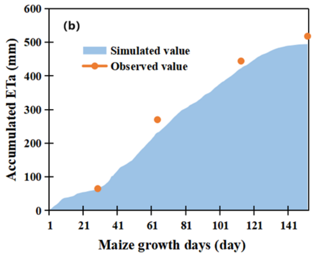

(b) T2

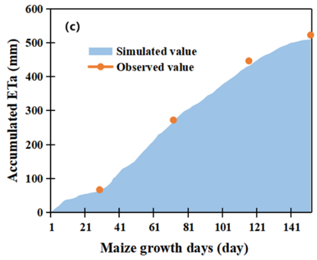

(c) T3

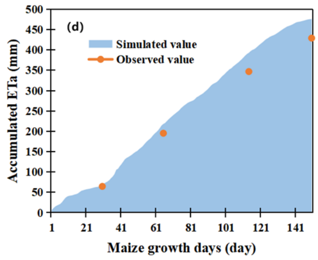

(d) T4

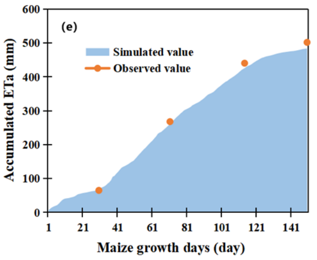

(e) T5

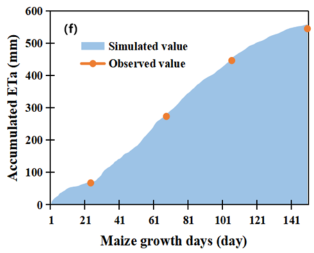

(f) T6

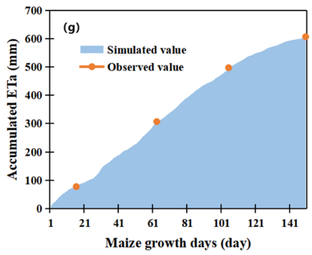

(g) T7

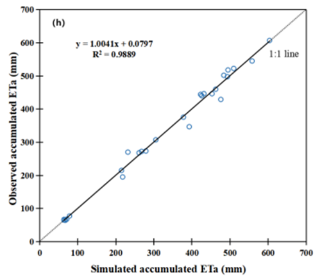

(h) T1-T7

Figure 4. Observational and simulated cumulative ET_a during the whole growth period of maize, (**a**) T1, (**b**) T2, (**c**) T3, (**d**) T4, (**e**) T5, (**f**) T6, (**g**) T7 and (**h**) calibration of ET_a for different stages (2014–2015).

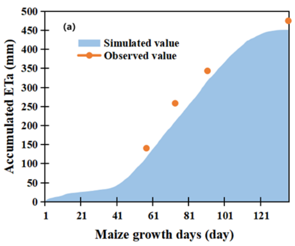

(a) T8

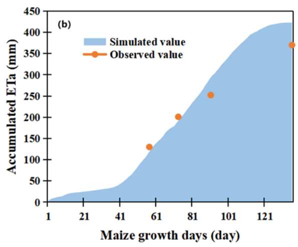

(b) T9

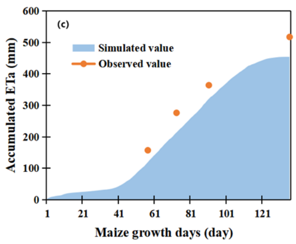

(c) T10

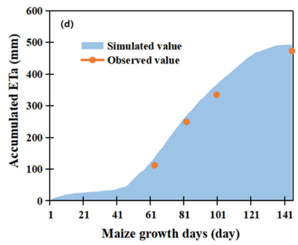

(d) T11

Figure 5. *Cont.*

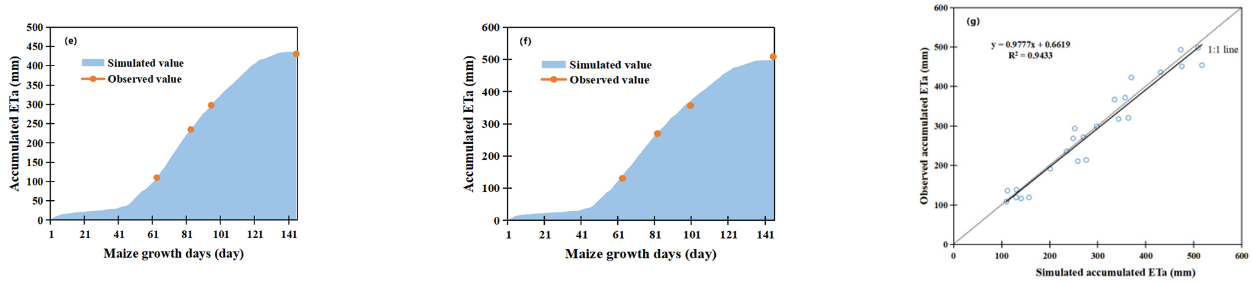

(e) T12 **(f)** T13 **(g)** T8-T13

Figure 5. Observational and simulated cumulative ET_a during the whole growth period of maize, **(a)** T8, **(b)** T9, **(c)** T10, **(d)** T11, **(e)** T12, **(f)** T13, and **(g)** validation of ET_a for different stages (2016–2017).

3.2. Projected Future Climate Change

Figure 6 presents the predicted future climate during the maize growing period. The highest *Pe*, *Tmax*, and *Tmin* appeared in the 2070s under the RCP4.5, they are 470.31 mm, 26.06 °C, and 14.69 °C, respectively, while the highest value of the *Rad* is 19.04 MJ/m^2 appeared at 2050s. In the RCP8.5, the average *Pe*, *Tmax* and *Tmin*, and *Rad* highest values appeared in the 2070s, they were 490.57 mm, 27.48 °C, 16.15 °C, and 19.08 MJ/m^2. RCP8.5's highest value of average *Pe*, *Tmax* and *Tmin*, and *Rad* was 4.31%, 5.45%, 9.94%, and 0.21% more than RCP4.5, respectively. Under the two RCPs, the maximum *Pe* appeared in the central and southern part of the study area; the highest *Rad* value mainly appears in the southwest. Moreover, the southern's *Tmin* has the highest value, and the *Tmax* high value was distributed in the southwestern and south.

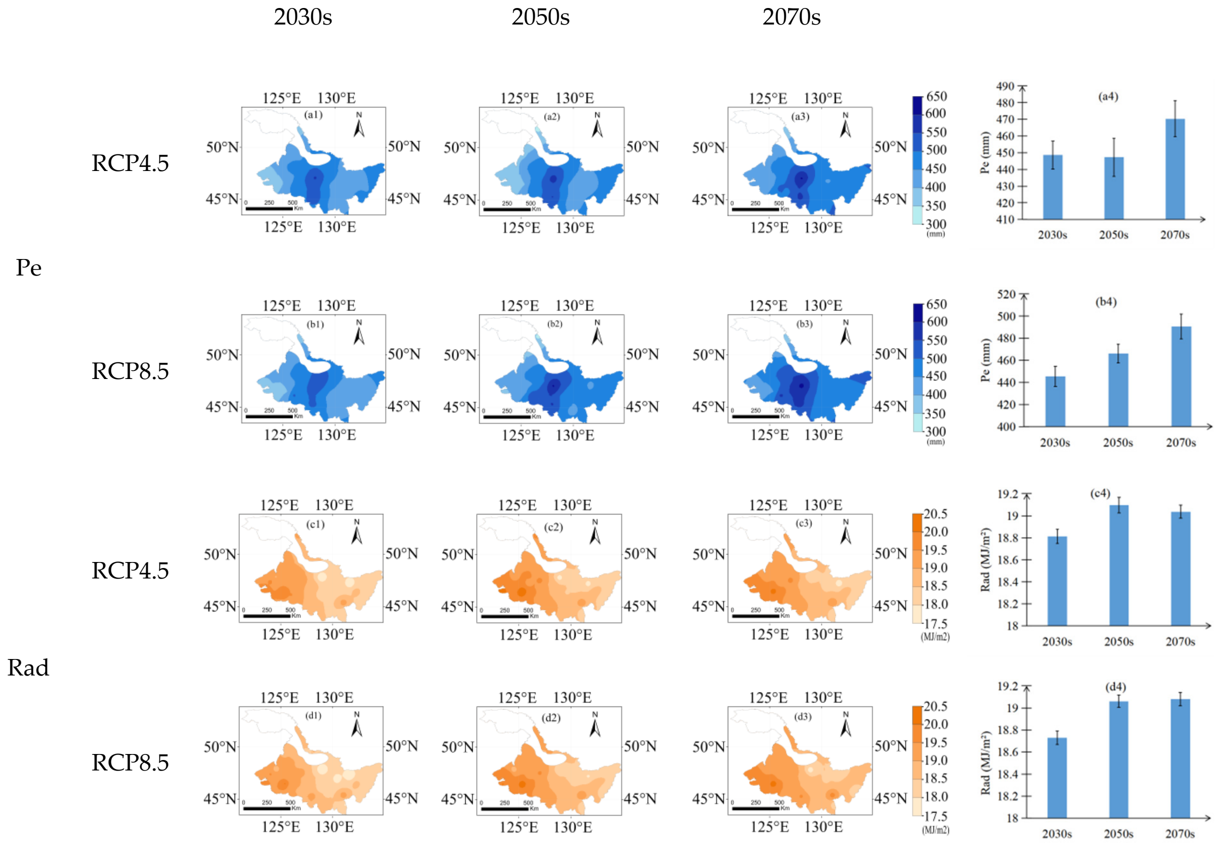

Figure 6. *Cont.*

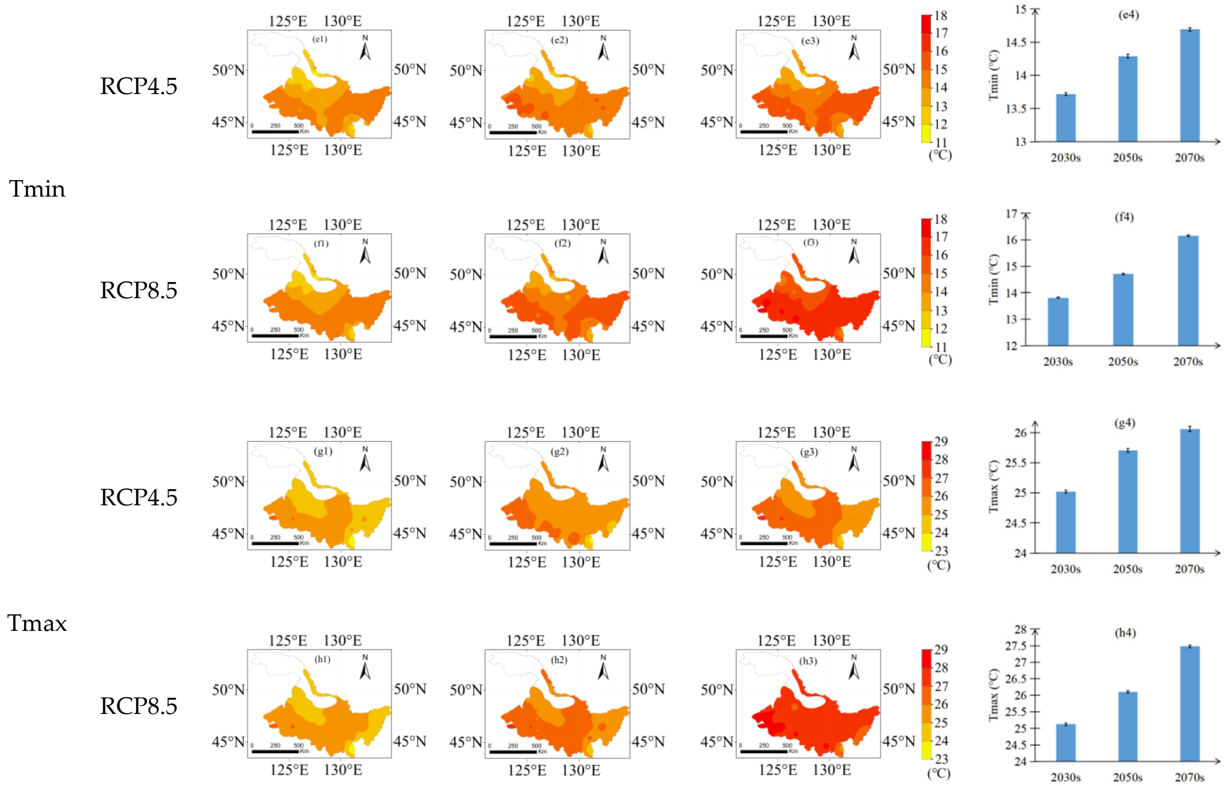

Figure 6. Spatial and temporal distribution of average precipitation (*Pe*) (**a1–a4**,**b1–b4**), solar radiation (*Rad*) (**c1–c4**,**d1–d4**), minimum temperature (*Tmin*) (**e1–e4**,**f1–f4**), and maximum temperature (*Tmax*) (**g1–g4**,**h1–h4**) for the multi-GCM ensemble during the maize growth stage under two RCPs from 2021–2080 in the study area.

3.3. ET_a Changes under Different Future Scenarios

The ET_a showed a declined trend from southwest to northeast in the study area (Figure 7). The ET_a had an upward trend under two RCPs with different magnitudes. The value of RCP8.5 is generally greater than the ET_a of RCP4.5. In the future, the maximum value of ET_a appears in the W3. Compared with the W3, W1, and W2 reduced by 1.5–1.6% and 0.4–0.6%.

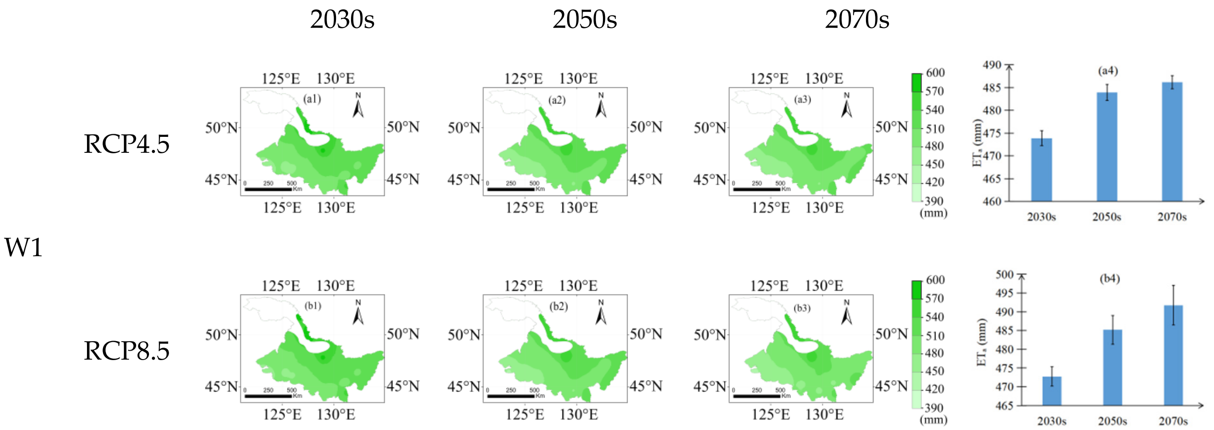

Figure 7. *Cont.*

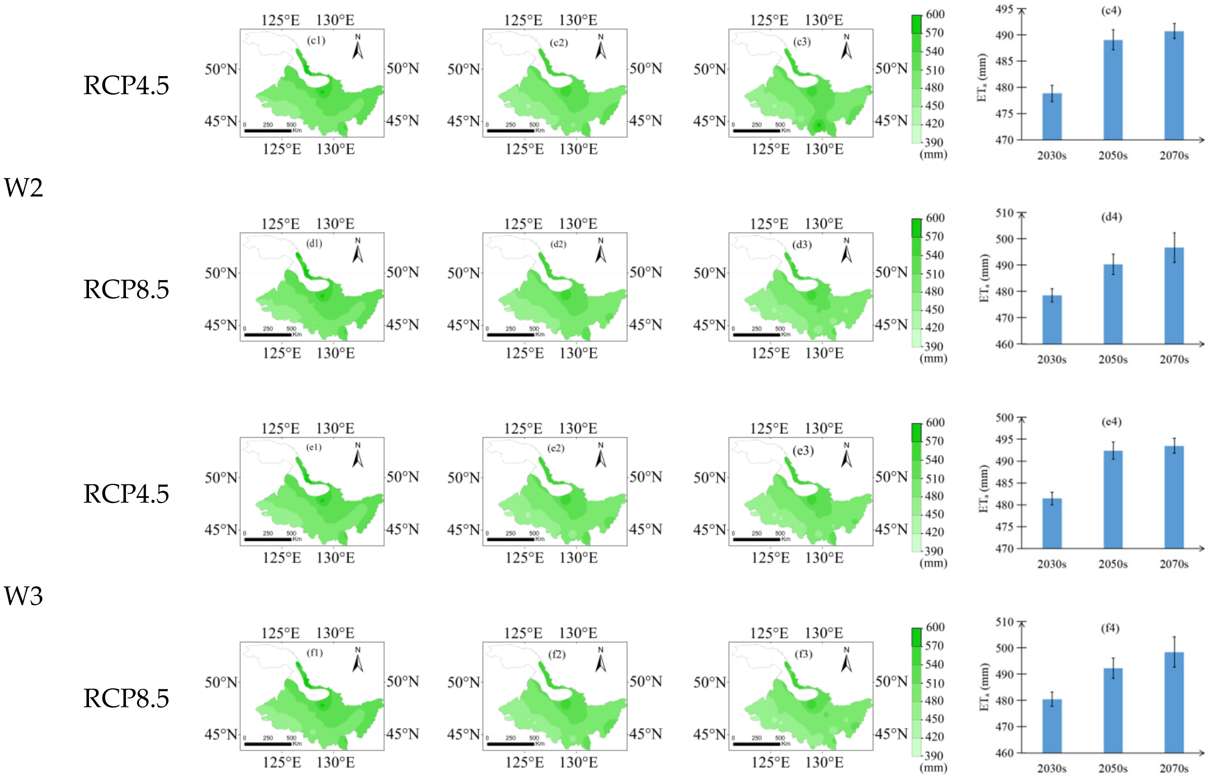

Figure 7. Spatial and temporal distribution of maize ET_a for the multi-GCM ensemble under different irrigation schedules ((**a1**–**a4**,**b1**–**b4**) W1, (**c1**–**c4**,**d1**–**d4**) W2,(**e1**–**e4**,**f1**–**f4**) W3) in the 2030s, 2050s, and 2070s with two RCPs.

3.4. Yield Changes under Different Future Scenarios

Maize yield under different irrigation schedules increased from the north part to the south area in the spatial distribution. The maximum value appeared in the southeast and southwest (Figure 8). Yield showed a growth trend from 2030s to 2070s. The maximum value for the three irrigation schedules appears in W3, which were 14,044 kg/ha (RCP4.5) and 14,402 kg/ha (RCP8.5).

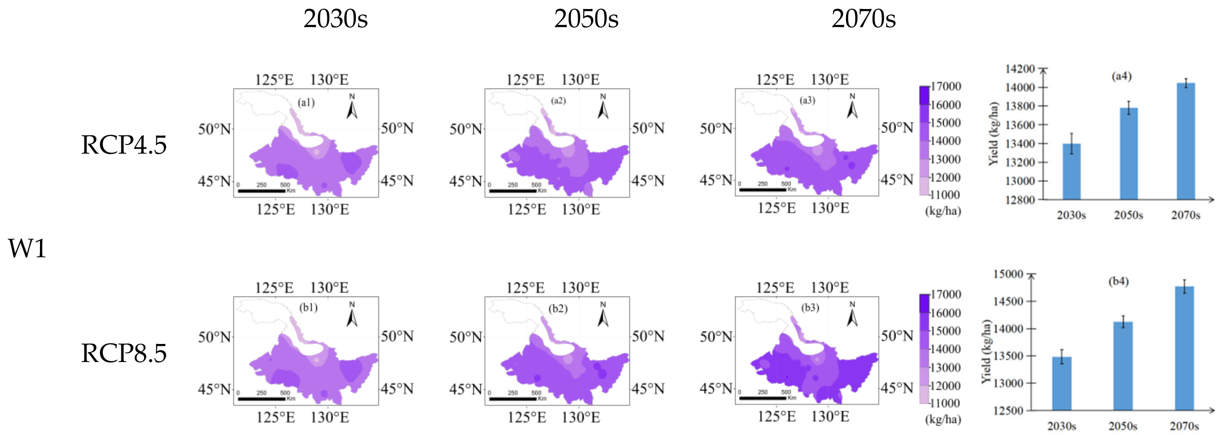

Figure 8. *Cont.*

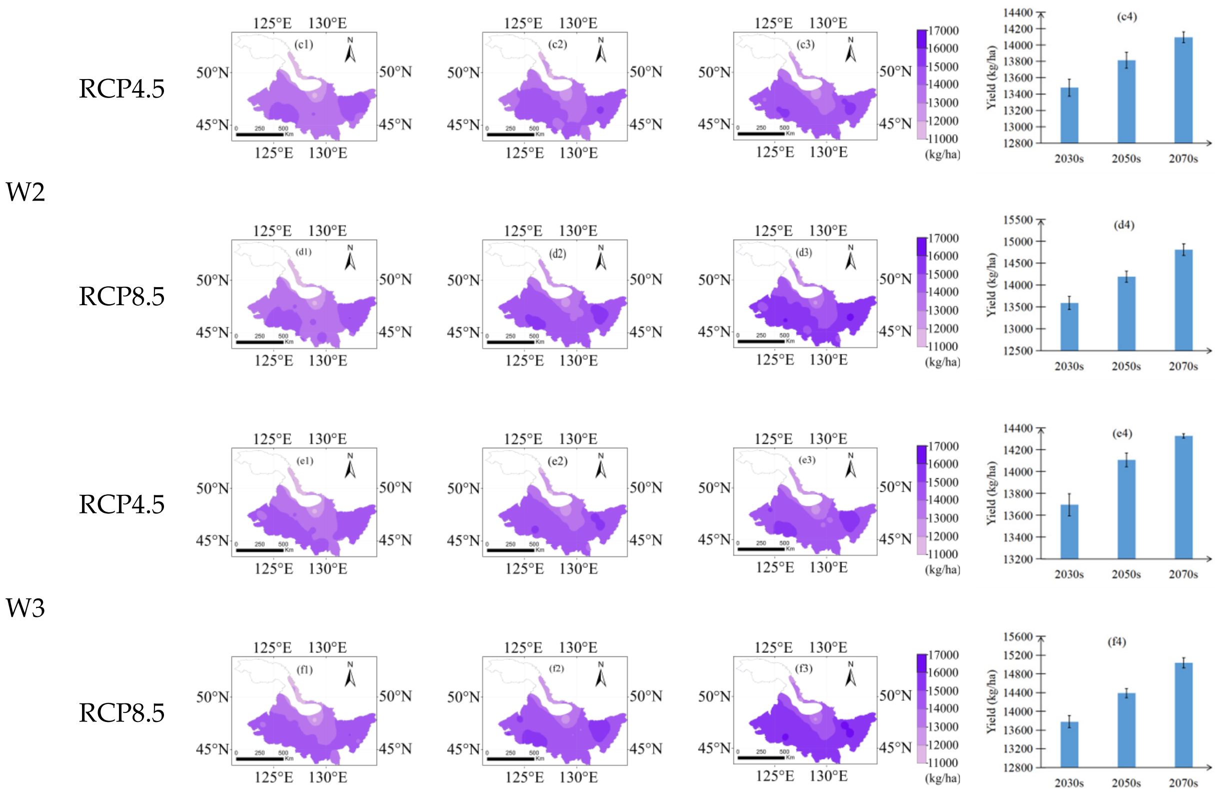

Figure 8. Spatial and temporal distribution of maize yield for the multi-GCM ensemble under different irrigation schedules ((**a1**–**a4**,**b1**–**b4**) W1,(**c1**–**c4**,**d1**–**d4**) W2,(**e1**–**e4**,**f1**–**f4**) W3) in the 2030s, 2050s, and 2070s with two RCPs.

3.5. WUE Changes under Different Future Scenarios

The *WUE* showed a growth trend from the west area to the east part (Figure 9). While the extent of increase in *WUE* under the two RCPs was different, and the RCP8.5′s *WUE* was larger than RCP4.5's. Under both of two RCPs, the minimum value of *WUE* appears in W2. Compared with W2, the *WUE* of the W1 and W3 increased by 0.5–0.6% and 0.9–1.2%.

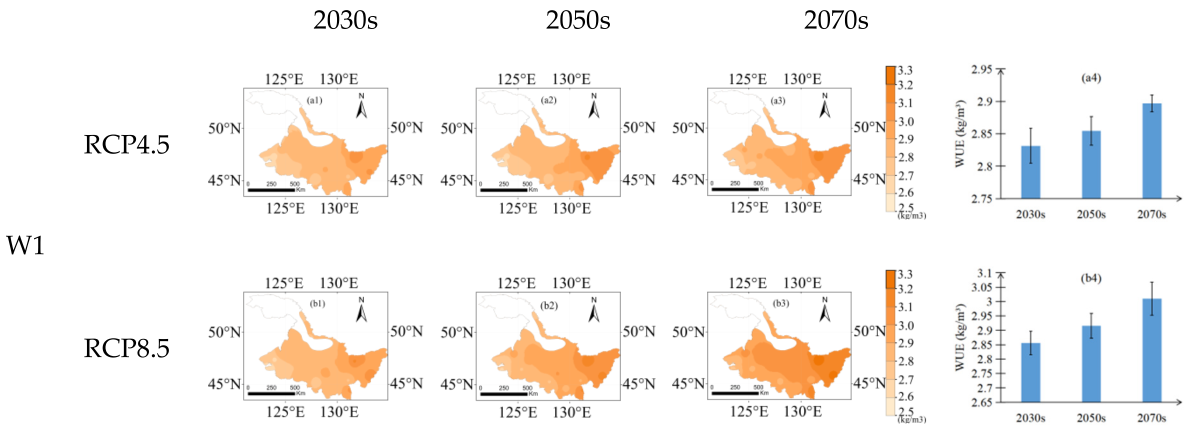

Figure 9. *Cont.*

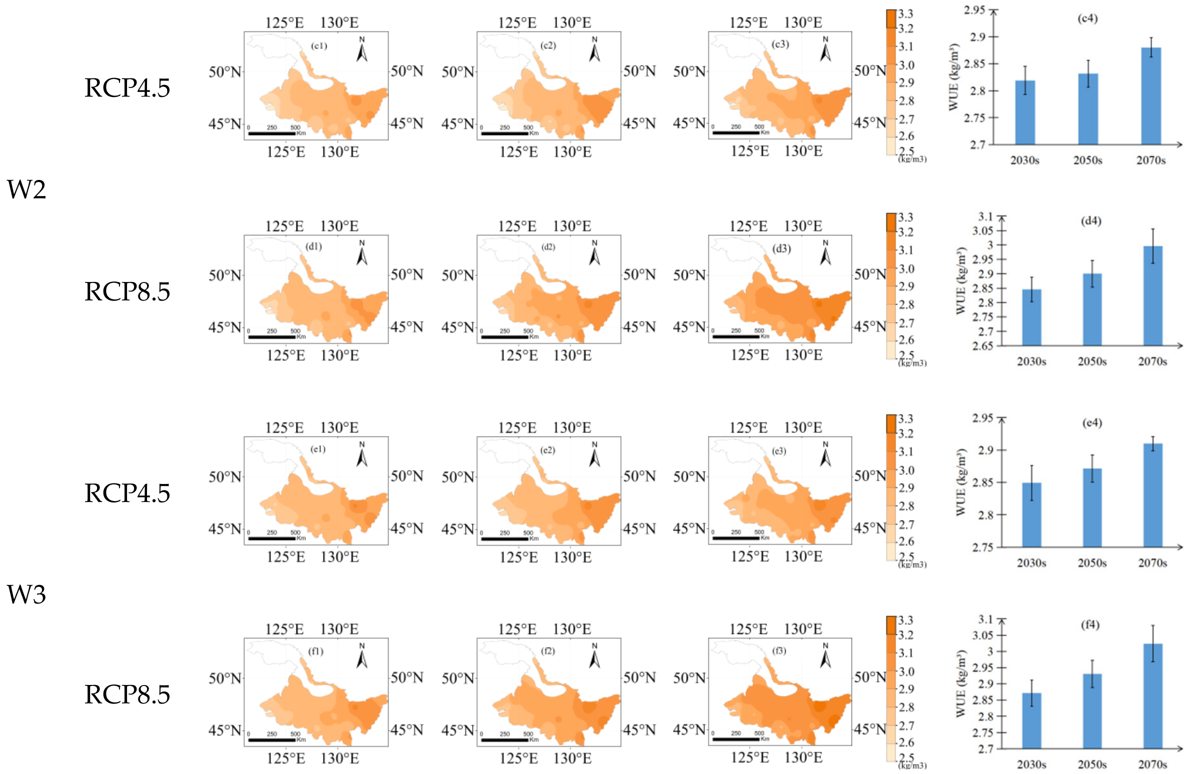

Figure 9. Spatial and temporal distribution of maize *WUE* for the multi-GCM ensemble under different irrigation schedules ((**a1–a4**,**b1–b4**) W1, (**c1–c4**,**d1–d4**) W2, (**e1–e4**,**f1–f4**) W3) in the 2030s, 2050s, and 2070s with two RCPs.

3.6. Assessment of Irrigation Optimization Scenarios and Corresponding Measures

Under the RCP4.5, the ET_a of W1, W2, and W3 were 481 mm, 486 mm, and 489 mm, respectively. The highest value of ET_a was in W3, and the lowest value was in W1. The difference between the three irrigation schedules is significant ($p \leq 0.05$) (Figure 10a). Yield under W3 was the highest. Although the W1's yield was less than W2's, the difference was not significant ($p > 0.05$) (Figure 11c). For *WUE*, W3's *WUE* was the highest among the three, and W1 and W2 were significantly lower than W3. Under the RCP8.5, the lowest value of ET_a appears in W1 ($p > 0.05$) (Figure 10b). Yields of maize under W1, W2, and W3 were 14,127kg/ha, 14,199 kg/ha, and 14,402 kg/ha, respectively. The results showed that the yield difference between W1 and W3 was significant ($p \leq 0.05$), and the yield difference between W2 and the other was not significant ($p > 0.05$) (Figure 11d). For *WUE*, W3 has the highest value. However, the difference between the three irrigation schedules is insignificant ($p > 0.05$). Overall, under the two RCPs, optimization selection W1 is recommended for farmers' reference as an optimal option under RDI, as W1 had a higher *WUE* without significantly decreasing yield.

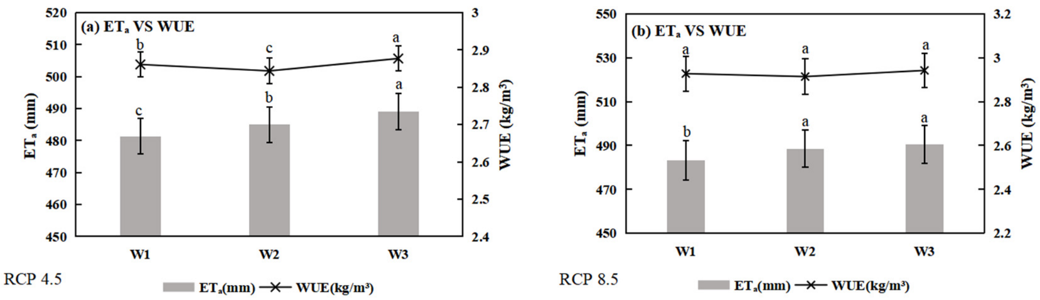

Figure 10. Relationship of *WUE* and ET_a under different irrigation optimization schedules. Different lowercase letters represent different levels of each column at $p \leq 0.05$.

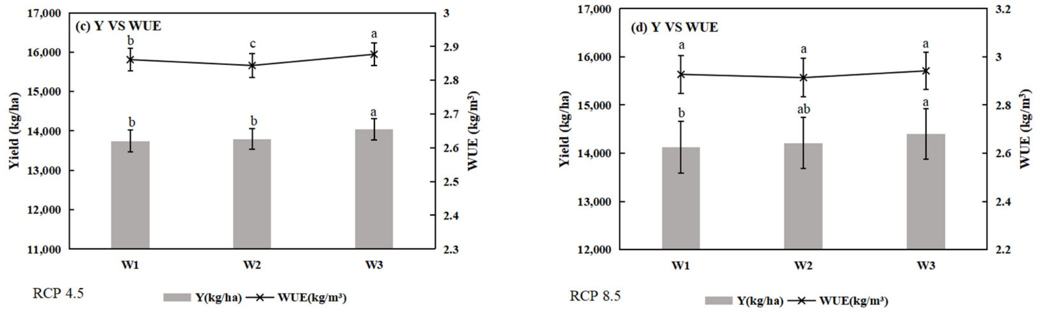

Figure 11. Relationship of Yield and *WUE* under different irrigation schedules. Different lowercase letters represent different levels of each column at $p \leq 0.05$.

4. Discussion

The four GCMs and two RCPs scenario models used in the study predicted an increase in temperature (*Tmin* and *Tmax*), *Pe*, and *Rad* in future study phases. Xiao et al. found that the crop growth stage would be shortened as the temperature increases. This condition usually reduces the transpiration of the crop during the growth stage [39]. The ET_a of most planting systems would somewhat decline with future climate change. Different ET_a would vary according to different cropping schedules under future climate scenarios [30]. Tao et al. [40] proposed that future temperature warming would significantly increase soil evaporation. Our results showed that ET_a increases as the temperature increases. The rising temperature may promote the photosynthesis and leaf expansion of crops, then accelerate the dry matter accumulation and crop growth, enhancing the transpiration, which is consistent with [41]. In this study area, the climate affected the southwestern Heilongjiang Province as a low-yield area. The relatively lower *Pe* and the higher ET_a, which may be due to the high temperature and *Rad*, leads to the lower *WUE* in this area. This study established analysis and comparison of irrigation schedules based on maize's different growth stages water stress. The results showed that maize's ET_a under treatments in which water stress appeared in the jointing stage was the least among all irrigation schedules. The reason may be that maize is more sensitive in the jointing stage with water stress. Jin et al. [42] indicated that maize's early growth stages were more vulnerable to water stress. The ET_a would reduce when water stress arises at filling stages. However, the results of this study were different from the result reported by Yu et al. [43]. They found that ET_a was the maximum when maize was exposed to water stress in the jointing stage. The results showed that photosynthesis in the early stage of maize growth was not only controlled by water stress, but the crop was still inhibited after rewatering, and it was difficult to recover. This result may be due to different research results obtained from other experimental locations. The degree of inhibition of crop growth is related to the duration of drought and the degree of stress. Future climate changes are complex, and the ET_a and yield of maize crops should be studied based on different future climate scenarios.

However, future climate changes would also affect maize yields. This climate change would impact crop yield and water supply and requirements. The increase in CO_2 concentration in the whole study area increases the possibility of photosynthesis and further promotes biomass accumulation in crops, thereby increasing yield [44,45]. This study showed that the RCP8.5's yield was higher than RCP4.5's, and the yield increased 386, 403, and 358 kg/ha under W1, W2, and W3, respectively. The results were similar to the results found by Qaisar et al. [46]. This study also showed that the yield under the RDI was lower than the yield under the full irrigation schedule, and the yield of W1 was lower than that of W2. This may be because the lack of development during the maize vegetative growth stage ultimately affects the reproductive development stage, and the high-quality output of ears and kernels reduces the yield of maize. Li et al. [47]'s research found that water decline leads to reduced leaf area, accelerated leaf senescence, and reduced photosynthesis, reducing leaf source activity and negatively affecting the seed setting rate, reducing maize yield. NeSmith et al. [48] proposed that the grain filling rate is not significantly affected by water deficit during grain filling. Therefore, our research results are consistent with theirs; the yield gap between W2 and W3 was not significant. Maize growth is a complicated process influenced by climatic, soil, and geographical factors, respectively [49]. Different irrigation schedules have less effect on the yield of maize, and the difference between them was not significant. Other researchers found that moderate water stress at the maize's jointing stage could increase crop *WUE* and control the growth redundancy of plants during the vegetative growth process, reduce the length of maize ears, and promote reproductive growth [50]. Cai et al. [51] and Wei et al. [52] found that appropriate water deficit treatments in the early stage of maize growth can improve crop *WUE* to varying degrees.

5. Conclusions

AquaCrop can simulate the maize ET_a and yield well, and the R^2 of the relationship between the model simulation and the observed were 0.99 and 0.71, respectively. Due to the increasing trend of future climate, the ET_a, yield, and *WUE* of maize in the two RCPs showed an increased trend during 2021–2080. The ET_a and yield showed an increasing trend from the north area to the south part in the study area, and *WUE* showed a downward trend from the east part to the west area. The ET_a, yield, and *WUE* of RCP8.5 were larger than these under RCP4.5. From the perspective of saving irrigation water without affecting the stability of maize yield, we recommend W1 for future maize planting. This study will supply useful knowledge with the impact of different irrigation schedules on crop growth under future climate, and help to optimize the selection of feasible irrigation schedules to balance the relationship between water scarcity and food security.

Author Contributions: T.N. collected the data; Y.T. and T.N. analyzed data; Y.T. wrote the paper; Y.T., N.L., Y.J. and T.W. drew the figures for this paper; Z.Z., P.C., T.L., C.D., S.Z. and Z.S. reviewed and edited this paper. All authors have read and agreed to the published version of the manuscript.

Funding: This work was fund by Basic Scientific Research Fund of Heilongjiang Provincial Universities [number: 2021-KYYWF-0019], Opening Project of Key Laboratory of Efficient Use of Agricultural Water Resources, Ministry of Agriculture and Rural Affairs of the People's Republic of China in Northeast Agricultural University [number: AWR2021002], National Natural Science Foundation Project of China [number: 51779046].

Data Availability Statement: Not applicable.

Acknowledgments: We thank the Chinese meteorological data sharing service (http://data.cma.cn, accessed on 30 March 2021) for providing the meteorological data. We thank all the members in Lab of Pumping, Hydraulic Teaching and Experimental Center of Heilongjiang University. Finally, we thank the anonymous reviewers and the editor for their suggestions, which substantially improved the manuscript.

Conflicts of Interest: The authors declare no conflict of interest.

References

1. Zhou, Y.; Li, N.; Dong, G.; Wu, W. Impact assessment of recent climate change on rice yields in the Heilongjiang Reclamation Area of north-east China. *J. Sci. Food Agric.* **2013**, *93*, 2698–2706. [CrossRef] [PubMed]
2. Piao, S.L.; Ciais, P.L.; Huang, Y.; Shen, Z.H.; Peng, S.S.; Li, J.S.; Zhou, L.P.; Liu, H.Y.; Ma, Y.C.; Ding, Y.H.; et al. The impacts of climate change on water resources and agriculture in China. *Nature* **2010**, *467*, 43–51. [CrossRef] [PubMed]
3. Ti, J.S.; Yang, Y.H.; Yin, X.G.; Liang, J.; Pu, L.L.; Jiang, Y.L.; Wen, X.Y.; Chen, F. Spatio-Temporal Analysis of Meteorological Elements in the North China District of China during 1960–2015. *Water* **2018**, *10*, 789. [CrossRef]
4. Intergovernmental Panel on Climate Change (IPCC). *Global warming of 1.5 °C: Impacts of 1.5 °C of Global Warming on Natural and Human Systems*; Contribution of Working Group I to the Sixth Assessment Report of the Intergovernmental Panel on Climate Change; IPCC Secretariat: Geneva, Switzerland, 2018.
5. Lin, Y.; Wenxiang, W.; Quansheng, G. CERES-Maize model-based simulation of climate change impacts on maize yields and potential adaptive measures in Heilongjiang Province, China. *J. Sci. Food Agric.* **2015**, *95*, 2838–2849. [CrossRef]
6. Fayaz, A.; Kumar, Y.R.; Lone, B.A.; Kumar, S.; Dar, Z.A.; Rasool, F.; Abidi, I.; Nisar, F.; Kumar, A. Crop Simulation Models: A Tool for Future Agricultural Research and Climate Change. *Asian J. Agric. Ext. Econ. Sociol.* **2021**, *39*, 146–154. [CrossRef]
7. Wang, W.; Peng, S.; Sun, F.; Xing, W.; Luo, F.; Xu, J. Spatialtemporal variations of rice irrigation water requirements in the mid-lower reaches of Yangtze River under changing climate. *Adv. Water Sci.* **2012**, *23*, 656–664. (In Chinese) [CrossRef]

8. Döll, P. Impact of climate change and variability on irrigation requirement: A global perspective. *Clim. Chang.* **2002**, *54*, 269–293. [CrossRef]
9. Tao, F.; Hayashi, Y.; Zhao, Z.; Sakamoto, T.; Yokozawa, M. Global warming, rice production, and water use in China: Developing a probabilistic assessment. *Agric. For. Meteorol.* **2008**, *148*, 94–110. [CrossRef]
10. Zheng, B.; Chenu, K.; Dreccer, M.; Chapman, S. Breeding for the future: What are the potential impacts of future frost and heat events on sowing and flowering time requirements for Australian bread wheat (Triticum aestivium) varieties? *Glob. Chang. Biol.* **2012**, *18*, 2899–2914. [CrossRef]
11. Kang, Y.; Khan, S.; Ma, X. Climate change impacts on crop yield, crop water productivity and food security—A review. *Prog. Nat. Sci.* **2009**, *19*, 1665–1674. [CrossRef]
12. Sun, H.; Zhang, X.; Liu, X.; Liu, X.; Shao, L.; Chen, S.; Wang, J.; Dong, X. Impact of different cropping systems and irrigation schedules on evapotranspiration, grain yield and groundwater level in the North China Plain. *Agric. Water Manag.* **2019**, *211*, 202–209. [CrossRef]
13. Aik, M.; Yetk, A.K.; Candoan, B.N.; Kuscu, H. Determining the yield responses of maize plant under different irrigation scenarios with AquaCrop model. *Int. J. Agric. Environ. Food Sci.* **2021**, *5*, 260–270. [CrossRef]
14. Sandhu, R.; Irmak, S. Performance of AquaCrop model in simulating maize growth, yield, and evapotranspiration under rainfed, limited and full irrigation. *Agric. Water Manag.* **2019**, *223*, 105687. [CrossRef]
15. Kang, S.Z.; Shi, W.J.; Hu, X.T.; Liang, Y.L. Effects of regulated deficit irrigation on physiological indexes and water use efficiency of maize. *Nongye Gongcheng Xuebao* **1998**, *4*, 83–87. (In Chinese)
16. Lv, P.P.; Lv, Z.D.; Bi, Y.J. Effects of regulated deficit irrigation with different irrigation amount on growth and yield of maize. *Glob. Water Resour. Dev. Manag.* **2020**, *2*, 9–13. (In Chinese) [CrossRef]
17. Trout, T.J.; Dejonge, K.C. Water productivity of maize in the US high plains. *Irrig. Sci.* **2017**, *35*, 251–266. [CrossRef]
18. Volk, J.; Gornott, C.; Sieber, S.; Lana, M.A. Can Tanzania's adaptation measures prevent future maize yield decline? A simulation study from Singida region. *Reg. Environ. Chang.* **2021**, *21*, 1–13. [CrossRef]
19. Jalil, A.; Akhtar, F.; Awan, U.K. Evaluation of the AquaCrop model for winter wheat under different irrigation optimization strategies at the downstream Kabul River Basin of Afghanistan. *Agric. Water Manag.* **2020**, *240*, 1–8. [CrossRef]
20. Heilongjiang Provincial People's Government. *Heilongjiang Yearbook*; Editorial Department: Harbin, China, 2020; pp. 244–245. ISSN 1008-0791.
21. Zhang, D.H.; Zhou, H.Q.; Lou, X. Problems and Countermeasures in Grain production in Heilongjiang Province. *Res. Agric. Mod.* **2012**, *33*, 411–414. (In Chinese)
22. Yang, C.Y.; Fraga, H.; Ieperen, W.V.; Santos, J.A. Assessment of irrigated maize yield response to climate change scenarios in Portugal. *Agric. Water Manag.* **2017**, *184*, 178–190. [CrossRef]
23. Cui, Y.; Lin, H.; Xie, Y.; Liu, S. Research on Application of AquaCrop Model in Crop Yield Prediction in Black Soil Region of Northeast China. *Sheng Tai Xue Bao* **2021**, *47*, 1–12. (In Chinese)
24. Abedinpour, M.; Sarangi, A.; Rajput, T.B.S.; Singh, M.; Pathak, H.; Ahmad, T. Performance evaluation of AquaCrop model for maize crop in a semi-arid environment. *Agric. Water Manag.* **2012**, *110*, 55–66. [CrossRef]
25. Shirazi, S.Z.; Mei, X.; Liu, B.; Liu, Y. Assessment of the AquaCrop Model under different irrigation scenarios in the North China Plain. *Agric. Water Manag.* **2021**, *257*, 107120. [CrossRef]
26. Abdalhi, M.A.M.; Jia, Z.H. Crop yield and water saving potential for AquaCrop model under full and deficit irrigation managements. *Ital. J. Agron.* **2018**, *13*, 1288. [CrossRef]
27. Nie, T.Z.; Jiao, Y.; Tang, Y.; Li, N.; Wang, T.Y.; Du, C.; Zhang, Z.X.; Li, T.C.; Zhu, S.J.; Sun, Z.Y.; et al. Study on the Water Supply and the Requirements, Yield, and Water Use Efficiency of Maize in Heilongjiang Province Based on the AquaCrop Model. *Water* **2021**, *13*, 2665. [CrossRef]
28. Adeboye, O.B.; Schultz, B.; Adeboye, A.P.; Adekalu, K.O.; Osunbitan, J.A. Application of the AquaCrop model in decision support for optimization of nitrogen fertilizer and water productivity of soybeans. *Inf. Process. Agric.* **2020**, *8*, 528–534. [CrossRef]
29. Wang, B.; Li, F.H.; Huang, Y.; Sun, Y.L.; Zhang, Z.X. Experimental Study on High Efficient Regulated Deficit Irrigation System for Maize in Cold Area and Black Soil Area. *J. Irrig. Drain.* **2013**, *32*, 113–115. (In Chinese) [CrossRef]
30. Xiao, D.; Liu, D.L.; Feng, P.; Wang, B.; Tang, J. Future climate change impacts on grain yield and groundwater use under different cropping systems in the North China Plain. *Agric. Water Manag.* **2021**, *246*, 106685. [CrossRef]
31. Liu, D.L.; O'Leary, G.J.; Christy, B.; Macadam, I.; Wang, B.; Anwar, M.R.; Weeks, A. Effects of different climate downscaling methods on the assessment of climate change impacts on wheat cropping systems. *Clim. Chang.* **2017**, *144*, 687–701. [CrossRef]
32. Yang, L.H.; Zhong, P.A.; Zhu, F.L.; Ma, Y.F.; Wang, H.; Li, J.Y.; Xu, C.J. A comparison of the reproducibility of regional precipitation properties simulated respectively by weather generators and stochastic simulation methods. *Stoch. Environ. Res. Risk Assess.* **2021**, *36*, 495–509. [CrossRef]
33. Nie, T.Z.; Zhang, Z.X.; Qi, Z.J.; Chen, P.; Sun, Z.Y.; Liu, X.C. Characterizing Spatiotemporal Dynamics of CH4 Fluxes from Rice Paddies of Cold Region in Heilongjiang Province under Climate Change. *Int. J. Environ. Res. Public Health* **2019**, *16*, 692. [CrossRef] [PubMed]
34. Moss, R.H.; Edmonds, J.A.; Hibbard, K.A.; Manning, M.R.; Rose, S.K.; Vuuren Van, D.P.; Carter, T.R.; Emori, S.; Kainuma, M.; Kram, T. The next generation of scenarios for climate change research and assessment. *Nature* **2010**, *463*, 747–756. [CrossRef] [PubMed]

35. Xiao, D.; Liu, D.; Wang, B.; Feng, P.; Tang, J. Climate change impact on yields and water use of wheat and maize in the North China Plain under future climate change scenarios. *Agric. Water Manag.* **2020**, *238*, 106238. [CrossRef]
36. Tavakoli, A.R.; Moghadam, M.M.; Sepaskhah, A.R. Evaluation of the AquaCrop model for barley production under deficit irrigation and rainfed condition in Iran. *Agric. Water Manag.* **2015**, *161*, 136–146. [CrossRef]
37. Nie, T.Z.; Zhang, Z.X.; Lin, Y.Y.; Chen, P.; Sun, Z.Y. Temporal and spatial distribution characteristics of corn water demand in Heilongjiang Province from 1959 to 2015. *Nongye Jixie Xuebao* **2018**, *49*, 217–227. (In Chinese) [CrossRef]
38. Bai, R.; Yan, H.L.; Xue, Y.M.; Yu, S.Q. The influence of climatic conditions on the growth and development of maize. *J. Agric. Catastrophol.* **2021**, *11*, 89–90. (In Chinese)
39. Xiao, D.P.; Tao, F.L. Contributions of cultivars, management and climate change to winter wheat yield in the North China Plain in the past three decades. *Eur. J. Agron.* **2014**, *52*, 112–122. [CrossRef]
40. Tao, F.L.; Xiao, D.P.; Zhang, S.; Zhang, Z.; Rotter, R.P. Wheat yield benefited from increases in minimum temperature in the Huang-Huai-Hai Plain of China in the past three decades. *Agric. For. Meteorol.* **2017**, *239*, 1–14. [CrossRef]
41. Zhang, J.P.; Wang, C.Y.; Yang, X.G.; Zhao, Y.X.; Liu, Z.J.; Wang, J.; Chen, Y.Y. Forecast of the impact of future climate change on corn water demand in the three provinces of Northeast China. *Nongye Gongcheng Xuebao* **2009**, *25*, 50–55. (In Chinese) [CrossRef]
42. Jin, N.; He, J.Q.; Fang, Q.; Chen, C.; Yu, Q. The Responses of Maize Yield and Water Use to Growth Stage-Based Irrigation on the Loess Plateau in China. *Int. J. Plant Prod.* **2020**, *14*, 621–633. [CrossRef]
43. Yu, W.Y.; Ji, R.P.; Feng, R.; Zhao, X.L.; Zhang, Y.S. Responses of maize leaf photosynthetic characteristics and water use efficiency to water stress in different growth stages. *Acta Ecol. Sin.* **2015**, *9*, 2902–2909. (In Chinese) [CrossRef]
44. Araya, A.; Hoogenboom, G.; Luedeling, E.; Hadgu, K.M.; Kisekka, I.; Martorano, L.G. Assessment of maize growth and yield using crop models under present and future climate in southwestern Ethiopia. *Agric. For. Meteorol.* **2015**, *214*, 252–265. [CrossRef]
45. Dixit, P.N.; Telleria, R.; Khatibb, A.N.A.; Allouzi, S.F. Decadal analysis of impact of future climate on wheat production in dry Mediterranean environment: A case of Jordan. *Sci. Total Environ.* **2018**, *610*, 219–233. [CrossRef] [PubMed]
46. Saddique, Q.; Liu, D.L.; Wang, B.; Feng, P.Y.; Cai, H. Modelling future climate change impacts on winter wheat yield and water use: A case study in Guanzhong Plain, northwestern China. *Eur. J. Agron.* **2020**, *119*, 126113. [CrossRef]
47. Li, Y.; Tao, H.; Zhang, B.; Huang, S.; Wang, P. Timing of water deficit limits maize kernel setting in association with changes in the source-flow-sink relationship. *Front. Plant Sci.* **2018**, *9*, 01326. [CrossRef] [PubMed]
48. NeSmith, D.S.; Ritchie, J. Maize (Zea mays L.) response to a severe soil water-deficit during grain-filling. *Field Crops Res.* **1992**, *29*, 23–35. [CrossRef]
49. Cantore, V.; Lechkar, O.; Karabulut, E.; Sellami, M.H.; Albrizio, R.; Boari, F.; Stellacci, A.M.; Todorovic, M. Combined effect of deficit irrigation and strobilurin application on yield, fruit quality and water use efficiency of "cherry" tomato (*Solanum lycopersicum* L.). *Agric. Water Manag.* **2016**, *167*, 53–61. [CrossRef]
50. Sun, J.P.; Wei, Y.X.; Wang, Y.Y. Water-saving and Yield-increasing Effects of Regulated Deficit Irrigation of Corn in Western Heilongjiang. *J. Agric. Mech. Res.* **2016**, *38*, 186–190. (In Chinese) [CrossRef]
51. Cai, H.J.; Kang, S.Z.; Zhang, Z.H.; Chai, H.M.; Hu, X.T.; Wang, J. Research on the Optimal Time and the Degree of Regulated Deficit Irrigation for Crop. *Nongye Gongcheng Xuebao* **2000**, *3*, 24–27. (In Chinese) [CrossRef]
52. Wei, Y.X.; Ma, Y.Y.; Liu, H.; Zhang, Y.F.; Yang, J.M.; Zhang, Y. Drip Irrigation Maize Plant and Soil Moisture and Water-saving and Yield-increasing Effects under Regulated Deficit Irrigation. *Nongye Jixie Xuebao* **2018**, *49*, 253–260. (In Chinese) [CrossRef]